

Brushed Block Copolymer Micelles with pH-Sensitive Pendant Groups for Controlled Drug Delivery

Hyun Jin Lee • Younsoo Bae

Received: 1 April 2013 / Accepted: 10 April 2013 / Published online: 2 May 2013
© Springer Science+Business Media New York 2013

ABSTRACT

Purpose To investigate the effects of small aliphatic pendant groups conjugated through an acid-sensitive linker to the core of brushed block copolymer micelles on particle properties.

Methods The brushed block copolymers were synthesized by conjugating five types of 2-alkanone (2-butanone, 2-hexanone, 2-octanone, 2-decanone, and 2-dodecanone) through an acid-labile hydrazone linker to poly(ethylene glycol)-poly(aspartate hydrazide) block copolymers.

Results Only block copolymers with 2-hexanone and 2-octanone (PEG-HEX and PEG-OCT) formed micelles with a clinically relevant size (< 50 nm in diameter), low critical micelle concentration (CMC, < 20 μ M), and drug entrapment yields (approximately 5 wt.%). Both micelles degraded in aqueous solutions in a pH-dependent manner, while the degradation was accelerated in an acidic condition (pH 5.0) in comparison to pH 7.4. Despite these similar properties, PEG-OCT micelles controlled the entrapment and pH-dependent release of a hydrophobic drug most efficiently, without altering particle size, shape, and stability. The molecular weight of PEG (12 kDa *vs* 5 kDa) induced no change in pH-controlled drug release rates of PEG-OCT micelles.

Conclusion Acid-labile small aliphatic pendant groups are useful to control the entrapment and release of a hydrophobic drug physically entrapped in the core of brushed block copolymer micelles.

KEY WORDS block copolymers • drug delivery • nanoparticles • pH-controlled release • polymer micelles

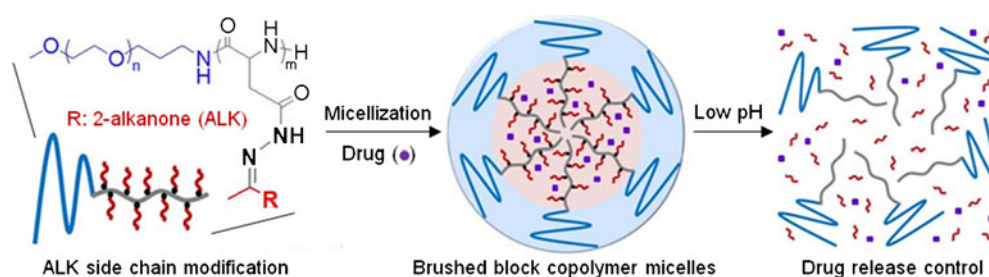
INTRODUCTION

Biocompatible nanoparticles have drawn attention for past decades as drug carriers for cancer treatment because they can improve water solubility of hydrophobic anticancer drugs and deliver the drugs preferentially to tumors (1–3). Compared to small molecule drugs, nanoparticles are too large to get removed through renal clearance, yet still small enough to pass through leaky tumor blood vessels, suppressing non-specific drug accumulation (4–7). Among such nanoparticle drug carriers, polymer micelles have been successfully used in several preclinical and clinical studies (8–10). Polymer micelles are spherical molecular assemblies from self-assembling block copolymers, and they are characterized by the nanoscale size (20–100 nm) and a well-defined core-shell structure. The micelles entrap various payloads, such as hydrophobic drugs, proteins, nucleotide drugs, and imaging agents in the core enveloped with a hydrophilic shell that suppress protein adsorption in the body (11–14).

Chemical conjugation and physical entrapment are two common methods for entrapping drug payloads in the micelles. For the chemical conjugation approach, micelle-forming polymers and drugs are often modified with degradable linkers. Ester, hydrazone, and carbonate are examples of such degradable linkers, which allow controlled release of drug in the body (15,16). *In vivo* signals, such as pH, redox reaction, and enzymatic activity, are used to degrade the linkers in a controlled manner (17,18). The physical entrapment approach is inevitable for drugs that do not have modifiable groups for chemical conjugation.

H. J. Lee • Y. Bae (✉)
Department of Pharmaceutical Sciences, College of Pharmacy,
University of Kentucky, 789 South Limestone,
Lexington, Kentucky 40536-0596, USA
e-mail: younsoo.bae@uky.edu

Fig. 1 Brushed block copolymer micelles for controlled release of hydrophobic drugs physically entrapped in the core.



Hydrophobic or ionic interactions are the driving forces of physical drug entrapment in many cases (19–21). The release of drugs physically entrapped in nanoparticles is time-dependent and controlled by modulating interactions between the drug and the nanoparticle core. The interactions often depend on lipophilicity, ionization, and morphology of the nanoparticle core (22–24). Many polymer micelles have been developed for either chemical conjugation or physical entrapment of the drug payloads separately, but each drug entrapment approach has its own advantage. For example, the chemical conjugation approach provides better control over drug release while the physical entrapment approach requires no chemical modification of the drug payload. A chemically modified drug is considered as a new compound that is completely different from the parent active pharmaceutical ingredient (API), and raises the use hurdle for approval of use in humans. Drug carriers entrapping unmodified APIs are expected to facilitate clinical translation. Therefore, combined use of chemical conjugation and physical entrapment approaches would improve polymer micelles as therapeutic tools more viable for clinical applications.

In this study, we tested our hypothesis that polymer micelles prepared from block copolymer with acid-sensitive pendant groups will control the release patterns of hydrophobic drugs physically entrapped in the micelles (Fig. 1). To test this hypothesis, we synthesized poly(ethylene glycol)-poly(aspartate hydrazide) block copolymer (PEG-HYD) to which 2-alkanone (ALK) with a different chain length was conjugated through an acid-labile hydrazone linker, and prepared polymer micelles loading a model anticancer drug (17-N-allylamino-17-demethoxygeldanamycin: 17-AAG) through physical entrapment. We have developed polymer micelles from PEG-HYD for pH-controlled drug delivery, which are compatible with other PEG-poly(aspartate) polymer micelles in several clinical studies (25–32). In our previous studies, we confirmed that PEG-HYD polymer micelles suppressed drug release in a physiological condition (pH 7.4) and accelerated drug release at an acidic pH (5.0) corresponding to intracellular lysosomes. Such an acid-accelerated drug release may be useful because tumor tissues are also acidic (pH < 7.0) due to the Warburg effect which explains inefficient consumption of glucose into energy in

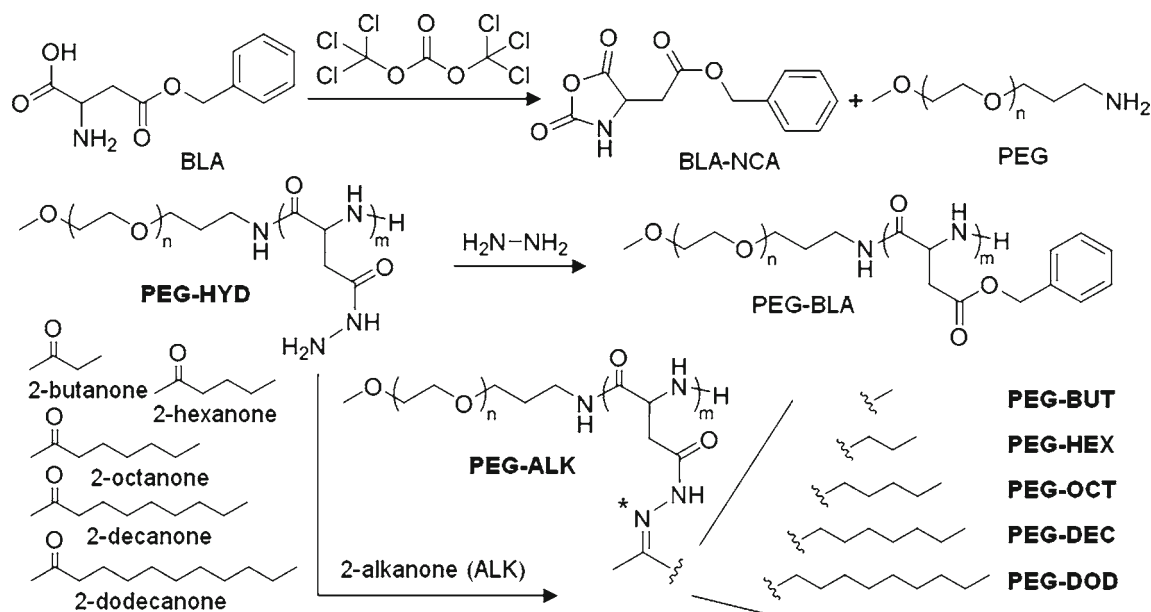
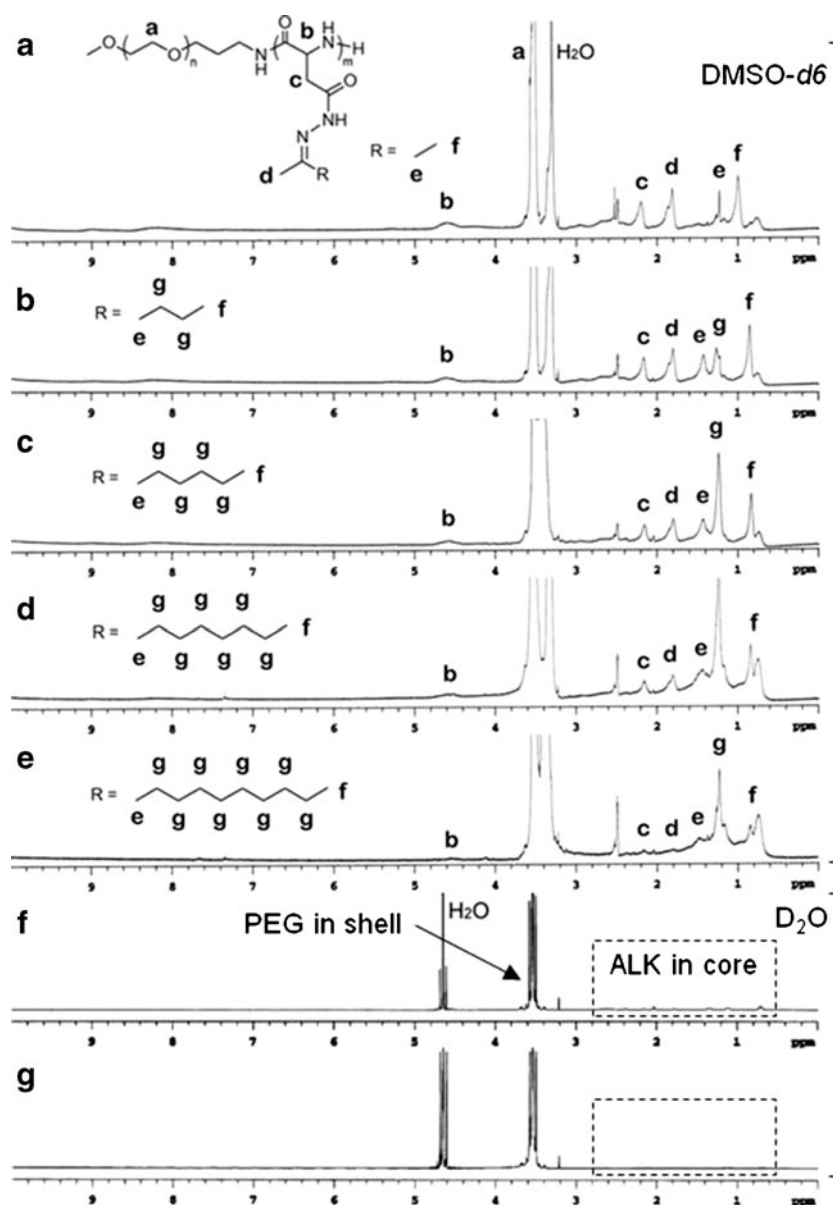


Fig. 2 Synthesis of PEG-ALK block copolymers.

Fig. 3 ^1H -NMR spectra of block copolymers: (a) PEG-BUT; (b) PEG-HEX; (c) PEG-OCT; (d) PEG-DEC; and (e) PEG-DOD; and micelles: (f) PEG-HEX; and (g) PEG-OCT.



cancer cells producing a large amount of lactic acids (18) and results in tumor acidosis (33). In addition to lysosomes, late endosomes are also acidic with pH ranging 5~6.5 (34). The

PEG-HYD micelles reduced toxicity of entrapped drugs by delivering the drug to tumor tissues preferentially and sparing normal tissues.

Fig. 4 Particle size distribution of PEG-HEX and PEG-OCT micelles.

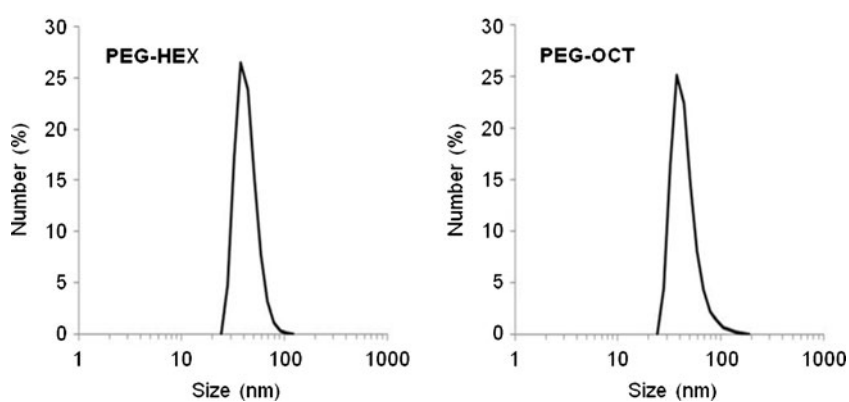
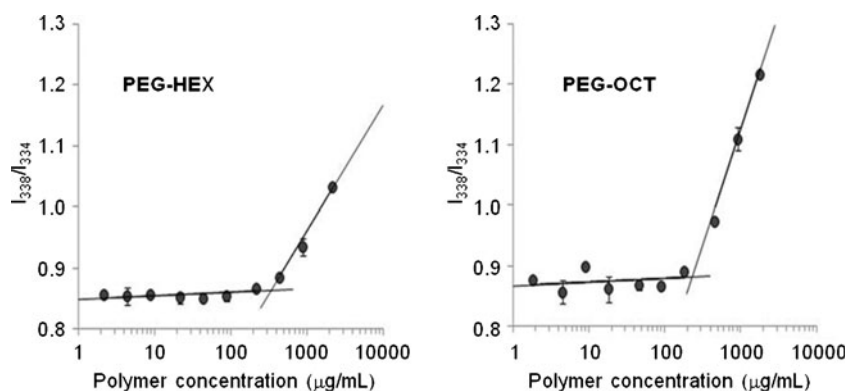


Fig. 5 Critical micelle concentrations of PEG-HEX and PEG-OCT micelles.



PEG-HYD was modified with ALK that has a ketone group on its 2 position and a different chain length to prepare polymer micelles from poly(ethylene glycol)-poly(aspartate hydrazide 2-alkanone) (PEG-ALK). As shown in Fig. 1, the PEG-ALK micelles were designed to degrade in an acidic condition and accelerate the release of physically entrapped drugs in a pH-dependent manner. To investigate the effects of the lipophilicity of ALK on drug entrapment and release patterns of the micelles, we evaluated five ALK compounds, including 2-butanone (BUT), 2-hexanone (HEX), 2-octanone (OCT), 2-decanone (DEC), and 2-dodecanone (DOD). PEG-ALK micelles were used to entrap 17-AAG, which is a potent inhibitor of 90 kDa heat shock protein that regulates expression of various oncoproteins in most tumor cells. Despite its unique mode of action, 17-AAG has low water solubility and requires the development of effective delivery tools (35–39).

MATERIALS AND METHODS

Materials

Following chemicals were purchased from Sigma-Aldrich (USA): L-aspartic acid β -benzyl ester (BLA), triphosgene,

anhydrous tetrahydrofuran (THF), anhydrous hexane, anhydrous dimethylsulfoxide (DMSO), anhydrous ethyl ether, anhydrous benzene, anhydrous hydrazine, BUT, HEX, OCT, DEC, DOD, acetonitrile (ACN), chloroform, dimethylsulfoxide- d_6 (DMSO- d_6), deuterium oxide (D_2O), pyrene, acetone, acetate buffer solutions, phosphate buffer solutions. α -Methoxy- ω -amino poly(ethylene glycol) (mPEG- NH_2) with molecular weight (MW) of 5 or 12 kDa was purchased from NOF Corporation (Japan). 17-AAG was purchased from LC Laboratories (USA). Regenerated cellulose dialysis bags with molecular weight cut off (MWCO) 6–8 kDa and Slide-A-Lyzer G2 dialysis cassettes with MWCO 10 kDa were purchased from Fisher Scientific (USA).

Synthesis of PEG-BLA Template Block Copolymers

A monomer, β -Benzyl-L-aspartate N-carboxy anhydride (BLA-NCA), was prepared for polymer synthesis by the Fuchs-Farthing method as previously reported (27,40). Briefly, BLA was reacted with triphosgene (1.3 molar equivalent) in dry THF under nitrogen at 45°C until the solution became clear. Anhydrous hexane was slowly added to the solution until NCA crystals appeared and disappeared quickly. The solution was recrystallized at -20°C overnight. BLA-NCA crystals were dried under vacuum. Ring-opening

Fig. 6 Particle size changes of PEG-HEX and PEG-OCT micelles in different pH conditions (7.4 and 5.0) at 37°C .

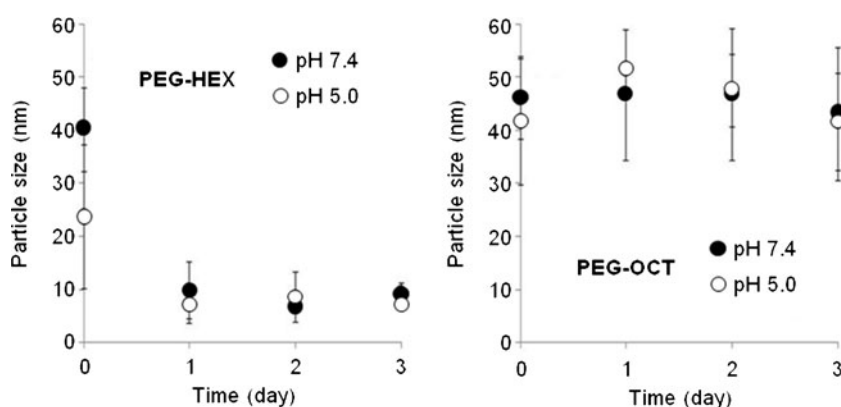
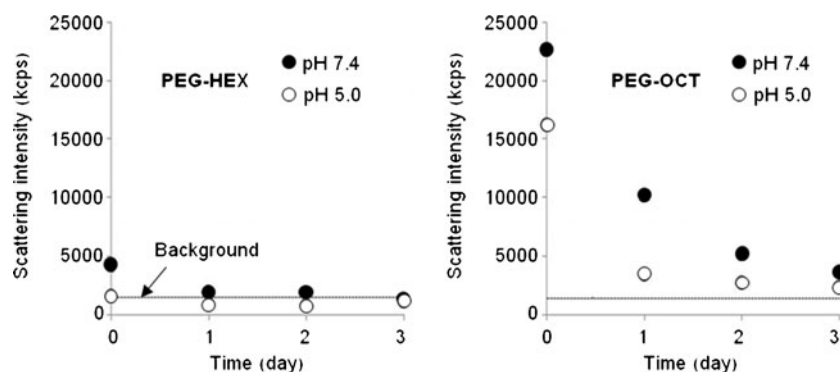


Fig. 7 Light scattering intensity changes of PEG-HEX and PEG-OCT micelles in different pH conditions (7.4 and 5.0) at 37°C.



polymerization of BLA-NCA was conducted by using mPEG-NH₂ (12 kDa or 5 kDa) as an initiator to prepare poly(ethylene glycol)-poly(β -benzyl L-aspartate) block copolymer (PEG-BLA) in anhydrous DMSO at 40°C for 2 days. PEG-BLA in the reaction solution was precipitated in ether and collected by freeze drying from benzene. Proton nuclear magnetic resonance (¹H-NMR, Varian, 500 MHz) was used to determine the composition of PEG-BLA.

Synthesis of PEG-ALK Micelles

The benzyl groups of PEG-BLA were replaced with hydrazide through aminolysis reaction to obtain PEG-HYD block copolymers. Excess hydrazine with respect to the number of BLA repeating units (10 fold) was reacted with PEG-BLA in DMSO at 40°C for 1 h. The product was purified through repetitive ether precipitation and collected by freeze drying. PEG-ALK was obtained after conjugation of various ALKs to PEG-HYD through a hydrazone bond (Fig. 2). For example, PEG-HYD was dissolved in DMSO and reacted with 2 fold of BUT with respect to the repeating HYD units to prepare PEG-BUT. After the reaction at room temperature for 48 h, final products were purified through repetitive ether precipitation and collected by freeze drying. PEG-HEX, PEG-OCT, PEG-DOC, and PEG-DOD were prepared by the same method. ¹H-NMR was used to confirm the synthesis of these polymers. PEG-ALK micelles

were then prepared by the oil-in-water method. For example, PEG-ALK (20 mg) was dissolved in DMSO (2 mL) first, and added dropwise to 8 mL deionized water under vigorous stirring. The solution was dialyzed against deionized water and freeze dried.

Critical Micelle Concentration (CMC) Measurements

A serial dilution of PEG-ALK micelles was prepared in aqueous solutions at various concentrations ranging 2 μ g/mL to 2 mg/mL. Each solution (200 μ L) was transferred in the wells of a 96-well plate, and mixed with pyrene in acetone (2 μ L, 30 μ M). The plate was incubated at a room temperature under a dark condition overnight prior to measuring the fluorescence of pyrene. Excitation spectra of pyrene incubated with micelles were observed by fluorescence spectroscopy (SpectraMax M5, Molecular Devices) with emission at 390 nm. The ratio between intensities at 334 nm and 338 nm (intensity ratio, I₃₃₄/I₃₃₈) was determined for each sample in triplicate.

Determination of PEG-ALK Micelle Degradation in Different pH Conditions

PEG-ALK micelles were prepared at 2 mg/mL in a phosphate buffer solution (10 mM, pH 7.4) or acetate buffer solution (10 mM, pH 5.0). All micelle solutions were passed through a 0.22 μ m filter prior to further characterization.

Fig. 8 GPC spectra of PEG-HEX and PEG-OCT micelles incubated in different pH conditions (7.4 and 5.0) at 37°C for 24 h.

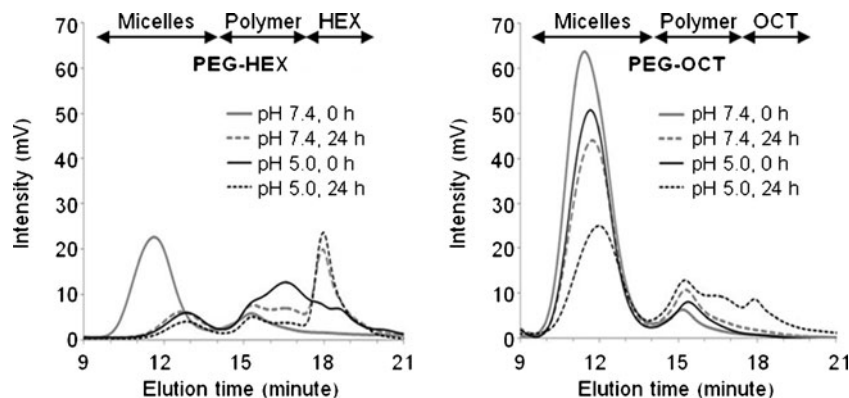
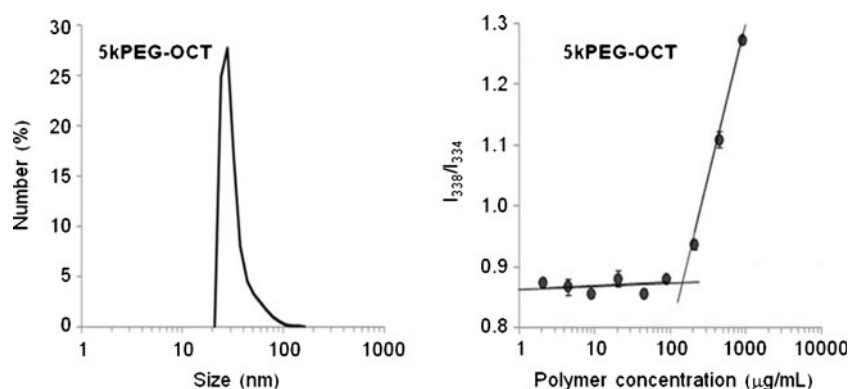


Fig. 9 Effects of PEG molecular weight on particle size and the CMC of PEG-OCT micelles.



Particle size and light-scattering intensity were determined by using a dynamic light scattering (DLS) detector (Zetasizer Nano 90, Malvern). Data were collected for 3 days while incubating the micelles at pH 7.4 or 5.0, 37°C. The micelle degradation was also confirmed with gel permeation chromatography (GPC) equipped with RI and UV detectors (Shimadzu LC20, PEG standard, 1× PBS saline mobile phase).

17-AAG Entrapment in PEG-ALK Micelles

PEG-ALK and 17-AAG were dissolved in DMSO and mixed for 30 min. The mixed solution (2 mL) was titrated to deionized water (6 mL) under vigorous stirring. Precipitates were removed by centrifuge, and the clear supernatant of drug-loaded micelles was dialyzed against deionized water to remove DMSO. The micelles were collected by freeze drying. A drug entrapment yield was determined by UV–vis spectroscopy (SpectraMax M5, Molecular Devices) at 365 nm, and expressed as weight % (wt%) of drugs in micelles.

Drug Release Experiments

Drug release experiments were conducted under the sink condition following the dialysis methods previously reported with slight modification (41–44). Drug-loaded micelles in deionized water (2 mg/mL) were put in six dialysis cassettes (MWCO 10 kDa). Three dialysis cassettes were placed in containers filled

with releasing media (buffer solutions at pH 7.4 or 5.0) at 37°C for 24 h while gentle magnetic stirring. To ensure drug diffusion from the dialysis cassette to the releasing medium was constant, the volume (5 L) of the releasing medium was maintained 3,000 times greater than the volume of the micelle solution in each dialysis cassette (1.5 mL). Drugs remaining in the dialysis cassette were measured at 0, 1, 3, 6 and 24 h. Data were expressed as means ± SD ($n=3$). The drug release was analyzed by using the first order kinetics model, $C_t/C_0 = e^{-kt}$ where C_t/C_0 is the proportion of the concentration drug remaining (C_t) at a given time (t) with respect to the initial drug concentration (C_0), and k is the first-order rate constant of drug release.

RESULTS AND DISCUSSION

Synthesis of PEG-ALK Micelles

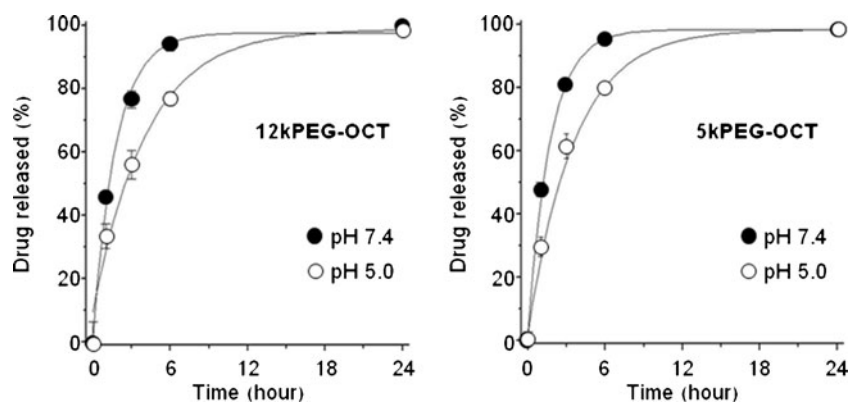
PEG-HYD and PEG-ALK were prepared as shown in Fig. 2. PEG-HYD was used to prepare all types of PEG-ALK to keep the composition of polymer backbone consistent. ^1H -NMR data show that PEG-HYD with 12 kDa PEG and 33 HYD units was successfully conjugated with five different ALK pendant groups (BUT, HEX, OCT, DEC, and DOD in Fig. 3a–e, respectively). PEG-HEX and PEG-OCT micelles showed predominant PEG peaks in D_2O (Fig. 3f and g), suggesting that these block copolymers self-assembled to form a core enveloped with a PEG shell. PEG-HEX micelles

Table 1 Characterization of PEG-ALK Micelles

Block copolymer	CMC (μM)	Size (nm)		17-AAG entrapment (wt %)	First-order drug release rate constant, k (h^{-1}) ^a	
		Blank micelles	17-AAG-entrapped micelles		pH 7.4	pH 5.0
PEG-HEX 12-33	17.1	43.9 ± 7.4	36.9 ± 8.0	0.77	—	—
PEG-OCT 12-33	11.6	45.8 ± 8.8	53.9 ± 3.2	4.9	0.252	0.469
PEG-OCT 5-33	10.9	42.8 ± 6.6	45.0 ± 3.6	4.2	0.277	0.506

^a Goodness of fitting (R^2) is 0.980–0.995

Fig. 10 Effects of PEG molecular weight on drug release profiles of PEG-OCT micelles.



however still show small peaks from the HEX segment (Fig. 3f). Molecular packing of PEG-HEX in the core might not be tight enough to suppress the magnetic resonance. In comparison, PEG-OCT micelles showed the PEG peak with no other peaks from OCT (Fig. 3g). These results indicate that PEG-OCT formed the micelles with the most hydrophobic core where polymer chains were tightly packed.

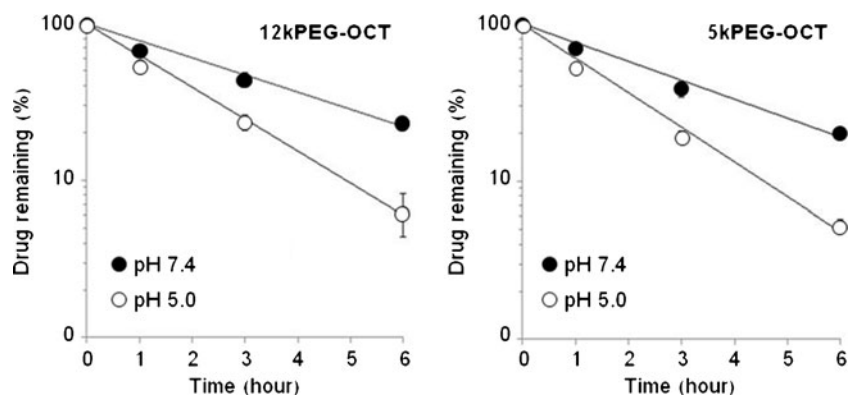
Despite the difference in core environment, both PEG-HEX and PEG-OCT micelles were similar in particle size (44 nm and 46 nm, respectively), showing a monodisperse distribution (Fig. 4). It must be noted that, among the five types of PEG-ALK, only PEG-HEX and PEG-OCT formed micelles. PEG-BUT, which had the shortest ALK pendant group, generated particles smaller than 10 nm in diameter, suggesting that BUT segments were not lipophilic enough to trigger self-assembling of block copolymers and form micelles. On the other hand, PEG-DEC and PEG-DOD with longer ALK pendant groups precipitated in aqueous solutions. We tested other methods to prepare micelles from PEG-DEC and PEG-DOD by using the dialysis or thin-film method with various organic solvents that effectively dissolved the polymer, such as DMSO, ACN, THF, and chloroform, but the attempts were unsuccessful. These results demonstrate that the degree of lipophilicity of PEG-ALK is important to prepare polymer micelles. Therefore, we selected PEG-HEX and PEG-OCT micelles for further characterization.

Particle stability of PEG-HEX and PEG-OCT micelles was characterized by measuring the CMC. As shown in Fig. 5, the pyrene intensity ratios (I_{338}/I_{334}) increased as the concentrations of PEG-HEX and PEG-OCT increased. Such changes demonstrate that PEG-HEX and PEG-OCT self-assemble into micelles, and the micelles have a core hydrophobic enough to entrap pyrene molecules. The CMCs determined from the breakpoint on the plot were 17.1 and 11.6 μM for PEG-HEX and PEG-OCT micelles, respectively. These results clearly demonstrate that PEG-OCT with more lipophilic ALK pendant groups can produce more stable micelles with a tightly packed core than PEG-HEX although both block copolymers have the same polymer backbone.

Degradation of PEG-ALK Micelles

PEG-HEX and PEG-OCT micelles were characterized to determine their particle stability in different pH conditions. Figure 6 shows that PEG-HEX micelles degraded into small pieces at pH 7.4 and 5.0 in 24 h. It is noticeable that PEG-HEX micelles degraded as soon as they were incubated at pH 5.0, while remaining stable at pH 7.4 in the initial stage of incubation. On the other hand, PEG-OCT micelles showed almost no degradation at both pH 7.4 and 5.0 for 3 days. Measurements of time-dependent changes in light scattering intensity revealed that PEG-OCT micelles also

Fig. 11 First-order kinetic analysis of drug release from 12kPEG-OCT and 5kPEG-OCT micelles.



degraded in aqueous solutions in a pH-dependent manner, although no change was observed in particle size. Figure 7 shows that light scattering intensity of PEG-HEX micelles decreased to the background level when the micelles were incubated at pH 5.0. This observation is consistent with the result in Fig. 6. On the other hand, the light scattering intensity of PEG-OCT micelles decreased gradually at pH 7.4 and 5.0 (Fig. 7). These results indicate that both PEG-HEX and PEG-OCT micelles can degrade pH-dependently in aqueous solutions, while PEG-OCT micelles slow down the rate of particle degradation in comparison to PEG-HEX micelles.

PEG-HEX and PEG-OCT micelles were prepared from the same PEG-HYD backbone, but they showed significantly different degradation patterns in aqueous solutions depending on the ALK pendant group attached. PEG-HEX micelles degraded instantly when they were exposed to an acidic solution, and the micelles dissociated completely even at pH 7.4 in 24 h. However, PEG-OCT micelles showed no changes in particle size although their light scattering intensity decreased gradually over 72 h. In order to understand the mechanism behind these observations, we conducted GPC analysis of the micelles in the process of degradation. Figure 8 clearly shows that three components are generated during the degradation process of PEG-HEX and PEG-OCT micelles, which include micelles, polymers and ALK pendant groups. In comparison to PEG-HEX that broke down to polymers and generated HEX, PEG-OCT micelles appeared primarily in the high molecular weight range on the GPC throughout the degradation process. These results suggest that PEG-OCT is hydrophobic enough to self-assemble into micelles with a smaller aggregation number of polymer chains per micelle.

One of the possible explanations for this phenomenon is that water molecules could get into the core of PEG-HEX micelles more effectively than that of PEG-OCT micelles, accelerating hydrolysis of ALK conjugation and ultimately particle degradation. ALK plays an important role in making the micelle core more hydrophobic and preventing water from triggering degradation of the acid-sensitive hydrazone in the core. PEG is another component that can modulate the amount of water surrounding the micelle core. To confirm the potential role of PEG on PEG-ALK micelle degradation, we prepared micelles from PEG-OCT with 5 kDa PEG (5kPEG-OCT micelles) and evaluated their particle stability in comparison to PEG-OCT with 12 kDa (12kPEG-OCT micelles). Figure 9 shows that the particle size (43 nm) and CMC (10.9 μ M) of 5kPEG-OCT micelles were similar to those of 12kPEG-OCT micelles. These results revealed that PEG does not affect particle stability of PEG-OCT micelles.

Loading and Release of 17-AAG Entrapment of PEG-ALK Micelles

PEG-OCT micelles with 5 and 12 kDa PEG were then used for entrapping 17-AAG to further evaluate their drug release patterns at different pH conditions. Drug entrapment yields were 4.9 and 4.2 wt.% for 12kPEG-OCT and 5kPEG-OCT, respectively. The drug loading in PEG-OCT micelles was significantly greater than that of PEG-HEX micelles (Table I). The extremely low drug loading (0.77 wt.%) in PEG-HEX micelles is unexpected from the result that PEG-HEX and PEG-OCT micelles showed similar CMCs. Nevertheless, these results indicate that drug entrapment is determined largely by the core environment rather than the molecular weight of PEG in PEG-OCT micelles.

Figure 10 shows drug release patterns of 12kPEG-OCT and 5kPEG-OCT micelles at pH 7.4 and 5.0. Interestingly, both micelles showed similar drug release patterns. The acid-accelerated release of 17-AAG is consistent with degradation patterns of PEG-ALK micelles. The drug release was analyzed further by using the first order kinetics model (Fig. 11 and Table I). The drug release rates were significantly different between pH 7.4 and 5.0, although there was no difference between 12kPEG-OCT and 5kPEG-OCT micelles. The release rate of PEG-OCT micelles ranged between 0.25~0.28 and 0.47~0.51 at pH 7.4 and 5.0, respectively. These data demonstrate that PEG-OCT micelles accelerated drug release by approximately 2 fold at pH 5.0 compared to pH 7.4. Obtained data also indicate that the effect of PEG shell on drug release from the PEG-OCT micelles is limited. Therefore, it is concluded that 17-AAG release from PEG-OCT micelles is dependent primarily on pH-dependent degradation of the core which is modulated by the type of ALK pendent groups attached to the core-forming segment of brushed block copolymer.

CONCLUSION

In this study, polymer micelles were prepared from brushed block copolymers (PEG-ALK) to which small aliphatic pendant groups with various chain lengths were conjugated through an acid-sensitive hydrazone linker. PEG-ALK block copolymers with HEX and OCT (PEG-HEX and PEG-OCT that possess 6 and 8 carbons, respectively) formed polymer micelles with a clinically relevant size (< 50 nm) and monodisperse distribution. $^1\text{H-NMR}$, DLS, and GPC analyses confirmed that PEG-OCT micelles underwent particle degradation in an acid-accelerated manner (pH 7.4 *vs* 5.0) while entrapping a model anticancer drug, 17-AAG (approximately 5 wt.%). Drug release from

PEG-OCT micelles was also accelerated in an acidic condition, which is in good agreement with the pH-dependent particle degradation pattern. The molecular weight of PEG induced no changes in drug entrapment and release patterns of PEG-OCT micelles. Taken together, these results conclude that small aliphatic pendant groups, conjugated to the core of brushed block copolymer micelles through an acid-sensitive linker, can control the entrapment and pH-dependent release of a hydrophobic drug entrapped physically in the micelle core. Therefore, this study provides a better understanding of the effect of core lipophilicity on physiochemical properties of block copolymer micelles that are designed to physically entrap a hydrophobic drug and degrade in a pH-dependent manner.

ACKNOWLEDGMENTS AND DISCLOSURES

This research is supported by the Kentucky Lung Cancer Research Program.

REFERENCES

- Davis ME, Chen Z, Shin DM. Nanoparticle therapeutics: an emerging treatment modality for cancer. *Nat Rev Drug Discov*. 2008;7:771–82.
- Duncan R. The dawning era of polymer therapeutics. *Nat Rev Drug Discov*. 2003;2:347–60.
- Peer D, Karp JM, Hong S, Farokhzad OC, Margalit R, Langer R. Nanocarriers as an emerging platform for cancer therapy. *Nat Nanotechnol*. 2007;2:751–60.
- Maeda H, Matsumura Y. Tumorotropic and lymphotropic principles of macromolecular drugs. *Crit Rev Ther Drug Carrier Syst*. 1989;6:193–210.
- Matsumura Y, Maeda H. A new concept for macromolecular therapeutics in cancer chemotherapy: mechanism of tumorotropic accumulation of proteins and the antitumor agent smancs. *Cancer Res*. 1986;46:6387–92.
- Takakura Y, Hashida M. Macromolecular carrier systems for targeted drug delivery: pharmacokinetic considerations on biodistribution. *Pharm Res*. 1996;13:820–31.
- Torchilin V. Tumor delivery of macromolecular drugs based on the EPR effect. *Adv Drug Deliv Rev*. 2011;63:131–5.
- Bae Y, Kataoka K. Intelligent polymeric micelles from functional poly(ethylene glycol)-poly(amino acid) block copolymers. *Adv Drug Deliv Rev*. 2009;61:768–84.
- Haag R. Supramolecular drug-delivery systems based on polymeric core-shell architectures. *Angew Chem Int Ed*. 2004;43:278–82.
- Mikhail AS, Allen C. Block copolymer micelles for delivery of cancer therapy: transport at the whole body, tissue and cellular levels. *J Control Release*. 2009;138:214–23.
- Kataoka K, Kwon GS, Yokoyama M, Okano T, Sakurai Y. Block-copolymer micelles as vehicles for drug delivery. *J Control Release*. 1993;24:119–32.
- Koo AN, Lee HJ, Kim SE, Chang JH, Park C, Kim C, *et al*. Disulfide-cross-linked PEG-poly(amino acid)s copolymer micelles for glutathione-mediated intracellular drug delivery. *Chem Commun*. 2008;6570–2.
- Lee HJ, Jang KS, Jang S, Kim JW, Yang HM, Jeong YY, *et al*. Poly(amino acid)s micelle-mediated assembly of magnetite nanoparticles for ultra-sensitive long-term MR imaging of tumors. *Chem Commun*. 2010;46:3559–61.
- Nasongkla N, Shuai X, Ai H, Weinberg BD, Pink J, Boothman DA, *et al*. cRGD-functionalized polymer micelles for targeted doxorubicin delivery. *Angew Chem Int Ed*. 2004;43:6323–7.
- Kratz F, Beyer U, Schutte MT. Drug-polymer conjugates containing acid-cleavable bonds. *Crit Rev Ther Drug Carrier Syst*. 1999;16:245–88.
- West KR, Otto S. Reversible covalent chemistry in drug delivery. *Curr Drug Discov Technol*. 2005;2:123–60.
- Lomaestro BM, Malone M. Glutathione in health and disease: pharmacotherapeutic issues. *Ann Pharmacother*. 1995;29:1263–73.
- Vander Heiden MG, Cantley LC, Thompson CB. Understanding the Warburg effect: the metabolic requirements of cell proliferation. *Science*. 2009;324:1029–33.
- Lee SC, Huh KM, Lee J, Cho YW, Galinsky RE, Park K. Hydro-tropic polymeric micelles for enhanced paclitaxel solubility: *in vitro* and *in vivo* characterization. *Biomacromolecules*. 2007;8:202–8.
- Saravanakumar G, Min KH, Min DS, Kim AY, Lee CM, Cho YW, *et al*. Hydrotropic oligomer-conjugated glycol chitosan as a carrier of paclitaxel: Synthesis, characterization, and *in vivo* biodistribution. *J Control Release*. 2009;140:210–7.
- Shin HC, Alani AW, Rao DA, Rockich NC, Kwon GS. Multi-drug loaded polymeric micelles for simultaneous delivery of poorly soluble anticancer drugs. *J Control Release*. 2009;140:294–300.
- Kim D, Gao ZG, Lee ES, Bae YH. *In vivo* evaluation of doxorubicin-loaded polymeric micelles targeting folate receptors and early endosomal pH in drug-resistant ovarian cancer. *Mol Pharm*. 2009;6:1353–62.
- Lee ES, Na K, Bae YH. Super pH-sensitive multifunctional polymeric micelle. *Nano Lett*. 2005;5:325–9.
- Yang SR, Lee HJ, Kim JD. Histidine-conjugated poly(amino acid) derivatives for the novel endosomolytic delivery carrier of doxorubicin. *J Control Release*. 2006;114:60–8.
- Alani AWG, Bae Y, Rao DA, Kwon GS. Polymeric micelles for the pH-dependent controlled, continuous low dose release of paclitaxel. *Biomaterials*. 2010;31:1765–72.
- Bae Y, Diezi TA, Zhao A, Kwon GS. Mixed polymeric micelles for combination cancer chemotherapy through the concurrent delivery of multiple chemotherapeutic agents. *J Control Release*. 2007;122:324–30.
- Bae Y, Fukushima S, Harada A, Kataoka K. Design of environment-sensitive supramolecular assemblies for intracellular drug delivery: polymeric micelles that are responsive to intracellular pH change. *Angew Chem Int Ed*. 2003;42:4640–3.
- Bae Y, Nishiyama N, Fukushima S, Koyama H, Yasuhiro M, Kataoka K. Preparation and biological characterization of polymeric micelle drug carriers with intracellular pH-triggered drug release property: tumor permeability, controlled subcellular drug distribution, and enhanced *in vivo* antitumor efficacy. *Bioconjug Chem*. 2005;16:122–30.
- Bae Y, Nishiyama N, Kataoka K. *In vivo* antitumor activity of the folate-conjugated pH-sensitive polymeric micelle selectively releasing adriamycin in the intracellular acidic compartments. *Bioconjug Chem*. 2007;18:1131–9.
- Matsumoto S, Christie RJ, Nishiyama N, Miyata K, Ishii A, Oba M, *et al*. Environment-responsive block copolymer micelles with a disulfide cross-linked core for enhanced siRNA delivery. *Biomacromolecules*. 2009;10:119–27.

31. Matsumura Y. Poly (amino acid) micelle nanocarriers in preclinical and clinical studies. *Adv Drug Deliv Rev.* 2008;60:899–914.
32. Ponta A, Bae Y. PEG-poly(amino acid) block copolymer micelles for tunable drug release. *Pharm Res.* 2010;27:2330–42.
33. Gillies RJ, Robey I, Gatenby RA. Causes and consequences of increased glucose metabolism of cancers. *J Nucl Med.* 2008;49:24s–42s.
34. Lee ES, Gao ZG, Bae YH. Recent progress in tumor pH targeting nanotechnology. *J Control Release.* 2008;132:164–70.
35. Chandran T, Katragadda U, Teng Q, Tan C. Design and evaluation of micellar nanocarriers for 17-allylamino-17-demethoxygeldanamycin (17-AAG). *Int J Pharm.* 2010;392:170–7.
36. Onyuksel H, Mohanty PS, Rubinstein I. VIP-grafted sterically stabilized phospholipid nanomicellar 17-allylamino-17-demethoxy geldanamycin: a novel targeted nanomedicine for breast cancer. *Int J Pharm.* 2009;365:157–61.
37. Stravopodis DJ, Margaritis LH, Voutsinas GE. Drug-mediated targeted disruption of multiple protein activities through functional inhibition of the Hsp90 chaperone complex. *Curr Med Chem.* 2007;14:3122–38.
38. Won YW, Yoon SM, Sonn CH, Lee KM, Kim YH. Nano self-assembly of recombinant human gelatin conjugated with alpha-tocopheryl succinate for Hsp90 inhibitor, 17-AAG, delivery. *ACS Nano.* 2011;5:3839–48.
39. Xiong MP, Yanez JA, Kwon GS, Davies NM, Forrest ML. A cremophor-free formulation for tanespimycin (17-AAG) using PEO-b-PDLLA micelles: characterization and pharmacokinetics in rats. *J Pharm Sci.* 2009;98:1577–86.
40. Bae Y, Jang W-D, Nishiyama N, Fukushima S, Kataoka K. Multifunctional polymeric micelles with folate-mediated cancer cell targeting and pH-triggered drug releasing properties for active intracellular drug delivery. *Mol Biosyst.* 2005;1:242–50.
41. Kwon GS, Okano T. Polymeric micelles as new drug carriers. *Adv Drug Deliv Rev.* 1996;21:107–16.
42. Liu H, Farrell S, Uhrich K. Drug release characteristics of unimolecular polymeric micelles. *J Control Release.* 2000;68:167–74.
43. Siepmann J, Peppas NA. Modeling of drug release from delivery systems based on hydroxypropyl methylcellulose (HPMC). *Adv Drug Deliv Rev.* 2001;48:139–57.
44. Klose D, Delplace C, Siepmann J. Unintended potential impact of perfect sink conditions on PLGA degradation in microparticles. *Int J Pharm.* 2011;404:75–82.